Photon Physics at CMS

Jonathan Hollar[1]

[1]Lawrence Livermore National Laboratory, 3000 East Ave., Livermore, California, USA

The Large Hadron Collider will allow studies of $\gamma\gamma$ and photoproduction interactions at energies significantly higher than previous experiments, in both pp and heavy ion collisions. In this article, studies of the feasibility of measuring $\gamma\gamma \to \ell^+\ell^-$, $\gamma p \to \Upsilon p \to \ell^+\ell^- p$, and $\gamma A \to \Upsilon A \to \ell^+\ell^- A$ processes in early LHC data with the CMS detector are presented.

1 Introduction

Exclusive dilepton production in pp collisions at CMS can occur through the processes $\gamma\gamma \to \ell^+\ell^-$ and $\gamma p \to \Upsilon p \to \ell^+\ell^- p$. Due to its precisely known cross-section the QED $\gamma\gamma \to \ell^+\ell^-$ process is a potential candidate for absolute luminosity measurements at the LHC, if the experimental systematics can be controlled. The cross-section for the $\gamma p \to \Upsilon p \to \ell^+\ell^- p$ process is expected to be related to the generalised gluon density of the proton as $\sigma \sim [g(x)]^2$. The increasing gluon density at low values of the fractional momentum x leads to a predicted dependence of $\sigma \sim W^{1.7}$ in leading order perturbative QCD, where W is the γp centre-of-mass energy. This results in large predicted cross-sections at the LHC, which will probe values of $\langle W \rangle$ significantly higher than previous measurements in ep collisions [10, 9]. At higher luminosities, photon interactions will reach sufficient energies to probe a wide range of physics beyond the Standard Model, such as Supersymmetric $\gamma\gamma \to \tilde{\ell}^+\tilde{\ell}^-$ production [2, 3, 4, 5], anomalous gauge boson couplings in $\gamma\gamma \to W^+W^-$ [5, 6], and other exotic models [7, 8]. In addition, the $pp \to p\ell^+\ell^- p$ sample will serve as an alignment sample for proposed forward proton spectrometers [12].

In heavy ion collisions, the effective luminosity of photon interactions is enhanced by the large electromagnetic field of the nucleus: by a factor Z^4 in $\gamma\gamma$ interactions, and a factor Z^2 in photoproduction. This allows studies of higher-order QED effects in a strongly-interacting regime ($\alpha Z \sim 0.6$), and studies of nuclear PDF's in vector-meson photoproduction. The $\gamma\gamma \to \ell^+\ell^-$ and $\gamma A \to J/\psi A^{(*)} \to \ell^+\ell^- A^{(*)}$ processes have been observed at RHIC [13]; the higher energies of the LHC will also allow studies of $\gamma A \to \Upsilon A^{(*)} \to \ell^+\ell^- A^{(*)}$.

2 Exclusive $\gamma\gamma \to \ell^+\ell^-$ and $\gamma p \to \Upsilon p \to \ell^+\ell^- p$ in pp Collisions

A Monte Carlo study of the prospects for measuring $\gamma\gamma \to \ell^+\ell^-$ and $\gamma p \to \Upsilon p \to \ell^+\ell^- p$ at CMS with 100 pb^{-1} of integrated luminosity at $\sqrt{s} = 14$ TeV has been performed. At low instantaneous luminosities the rate of pileup (multiple interactions in the same bunch crossing) is expected to be small, meaning the signal can be distinguished by the presence of two leptons

and no other activity above the noise thresholds. Zero pileup is assumed throughout the current study.

Signal events are produced using the LPAIR [11] (for $\gamma\gamma \to \ell^+\ell^-$) and STARLIGHT [14] (for $\gamma p \to \Upsilon p \to \ell^+\ell^- p$) generators. The largest background after all selection criteria are applied are inelastic photon-exchange events, in which the proton remnants escape undetected. The other sources of dilepton backgrounds relevant to CMS include Drell-Yan production, quarkonium decays, and heavy-flavor semileptonic decays. The Pythia generator is used to generate all of these samples. Both signal and background samples are passed through a full detector simulation, trigger emulation, and reconstruction.

3 Event Selection

3.1 Trigger and Lepton Selection

As the signal consists primarily of very low p_T leptons, the lowest possible trigger thresholds are required to select a large sample of events. In the dimuon channel, the standard CMS dimuon trigger for a luminosity of $10^{32}\,\mathrm{cm}^{-2}\mathrm{s}^{-1}$ is assumed, requiring two muons with $p_T > 3$ GeV. In the dielectron channel, the threshold is lowered using a dedicated trigger. In the Level 1 (hardware) trigger, exactly two EM candidates and no additional jets with $p_T > 10$ GeV are required. In the High Level Trigger (HLT), the EM candidates are required to be matched to charged tracks, and to be back-to-back in ϕ and balanced in the transverse energy E_T.

Starting from the triggered sample of dileptons, we require that the offline reconstruction find exactly two same flavor opposite-sign dileptons in the event. Further selections on the acoplanarity ($|\Delta\phi(\ell^+\ell^-)|$) and transverse momentum balance ($|\Delta p_T(\ell^+\ell^-)|$) are applied, exploiting the constrained kinematics of the signal. In the $\mu^+\mu^-$ channel, we require $|\Delta\phi(\mu^+\mu^-)| > 2.9$ and $|\Delta p_T(\mu^+\mu^-)| < 2.0$ GeV. In the e^+e^- channel, we require $|\Delta\phi(e^+e^-)| < 2.7$ and $|\Delta E_T(e^+e^-)| < 5.0$ GeV.

3.2 Exclusivity Selection

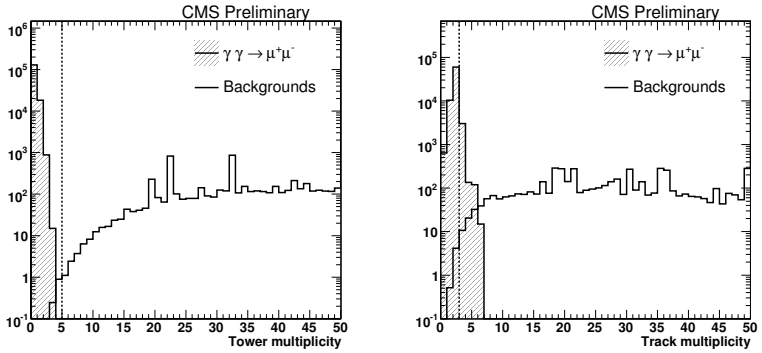

Figure 1: Multiplicity of extra calorimeter towers (left) and charged track multiplicity (right) for signal (shaded histogram) and background (open histogram), with arbitrary normalization.

In the no-pileup startup scenario assumed here, the signal is distinguished by having no calorimeter activity that is not associated with the leptons, and no charged tracks in addition to the two signal leptons. A common exclusivity selection is applied for the dimuon and dielectron channels.

The calorimeter exclusivity requirement is implemented by requiring there be no more than 5 "extra" calorimeter towers with $E > 5$ GeV, where extra towers are defined as those separated from either of the lepton candidates by $\Delta R > 0.3$ in the $\eta - \phi$ plane. The resulting distribution for the $\gamma\gamma \to \mu^+\mu^-$ signal and the sum of backgrounds are shown in Figure 1 (left).

The track exclusivity requirement provides additional background suppression in the $|\eta| < 2.5$ region covered by the tracker. The track multiplicity distributions for signal and background are shown in Figure 1 (right). We require the track multiplicity be $N(tracks) < 3$.

3.2.1 Forward Detector Vetos

Since inelastic photon-exchange events will have a high efficiency for passing the selection described in the previous sections, a veto on activity in the forward detectors is useful in suppressing these backgrounds. The ZDC (Zero Degree Calorimeter) detector covers the region $|\eta| > 8.2$, and will detect high energy neutrons and photons. The$CASTOR$ detector provides a nearly continuous extension of coverage from the hadronic calorimeter to the region $5.2 < |\eta| < 6.6$.

Since a full simulation and reconstruction is not yet available for these detectors, we estimate their ability to reject inelastic backgrounds based on their generator level acceptance. We assume a startup scenario in which a $CASTOR$ detector is available on one side of CMS only, and ZDC detectors are available on both sides. With these assumptions, approximately 2/3 of the remaining inelastic background can be vetoed using the combination of $CASTOR$ and ZDC.

4 Results

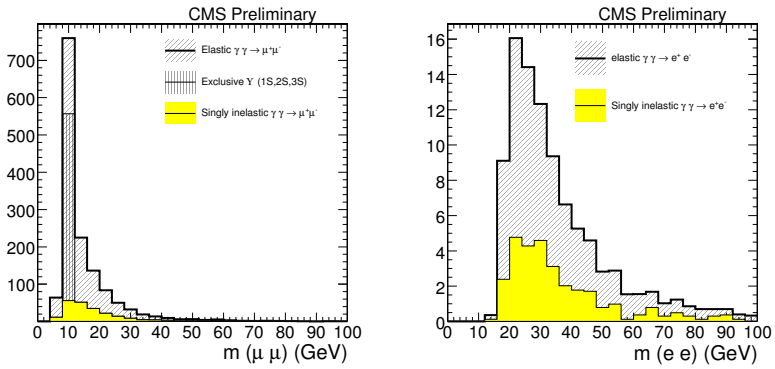

Figure 2: $m(\mu^+\mu^-)$ (left) and $m(e^+e^-)$ (right) for events passing all selection criteria. The elastic two-photon (open histogram) Υ photoproduction (shaded histogram), and singly inelastic background (solid histogram) are shown.

The dilepton invariant mass distributions after application of all trigger and selection criteria are shown in Figure 2. The expected elastic $\gamma\gamma \to \mu^+\mu^-$ signal yields in $100\,\mathrm{pb}^{-1}$ are:

$$N_{elastic}(\gamma\gamma \to \mu^+\mu^-) = 709 \pm 27,$$

where the statistical error is $\sqrt{N_{elastic}}$. The expected contribution from singly inelastic two-photon events, assuming the ZDC and CASTOR vetoes described previously, is:

$$N_{inelastic}(\gamma\gamma \to \mu^+\mu^-) = 223 \pm 15 \pm 42(\mathrm{model}),$$

where the first uncertainty is taken as $\sqrt{N_{inelastic}}$, and the second corresponds to a 19% model-dependent uncertainty on the inelastic cross-section. Without the ZDC and Castor vetoes, the singly inelastic contribution would be significantly larger:

$$N_{inelastic}(\gamma\gamma \to \mu^+\mu^-) = 636 \pm 25 \pm 121(\mathrm{model}),$$

where the errors are $\sqrt{N_{inelastic}}$ and model-dependence.

In the $\gamma\gamma \to e^+e^-$ channel, the expected yields are significantly smaller due to the higher trigger threshold and lower efficiency for reconstructing low E_T electrons. After all trigger and selection criteria are applied the expected elastic signal yields in $100\,\mathrm{pb}^{-1}$ are:

$$N_{elastic}(\gamma\gamma \to e^+e^-) = 67 \pm 8,$$

where the error is $\sqrt{N_{elastic}}$. The expected contribution from singly inelastic two-photon events, assuming the ZDC and CASTOR vetoes, is:

$$N_{inelastic}(\gamma\gamma \to e^+e^-) = 31 \pm 6 \pm 6(\mathrm{model}),$$

where the first uncertainty is $\sqrt{N_{inelastic}}$, the second corresponds to a 19% model-dependent uncertainty on the inelastic cross-section. Without the ZDC and CASTOR vetoes, the singly inelastic contribution would be:

$$N_{inelastic}(\gamma\gamma \to e^+e^-) = 82 \pm 9 \pm 15(\mathrm{model}),$$

where the errors are $\sqrt{N_{inelastic}}$ and model-dependence.

5 Applications

5.1 Luminosity Studies

The small theoretical uncertainty on the $\gamma\gamma \to \ell^+\ell^-$ cross-section makes it a candidate for use as an absolute luminosity normalization sample. Due the contribution of the theoretically less clean inelastic events, the elastic signal cannot be extracted on an event-by-event basis. However, the $\Delta\phi$ and Δp_T distributions provide a means of statistically separating the two contributions. This is shown in Figure 3 for the sample of $\gamma\gamma \to \mu^+\mu^-$ events passing all selection requirements.

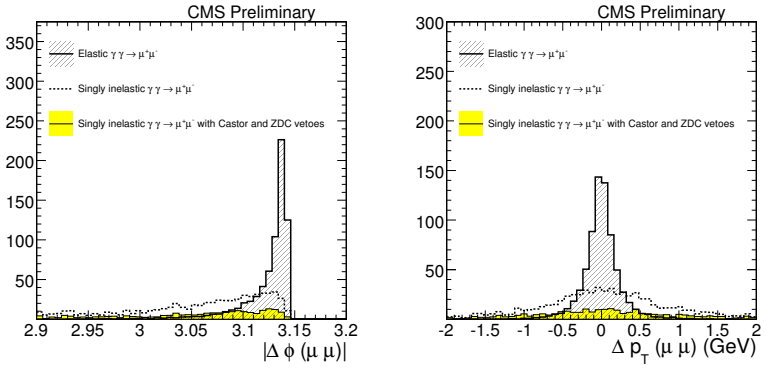

Figure 3: Distributions of $|\Delta\phi(\mu^+\mu^-)|$ (left) and $|\Delta p_T(\mu^+\mu^-)|$ (right) for $\gamma\gamma \to \mu^+\mu^-$ events passing all selection requirements. The elastic signal is denoted by the open histogram, the inelastic background is shown with no $CASTOR/ZDC$ vetos (dashed line), and with the vetos described in the text (solid histogram).

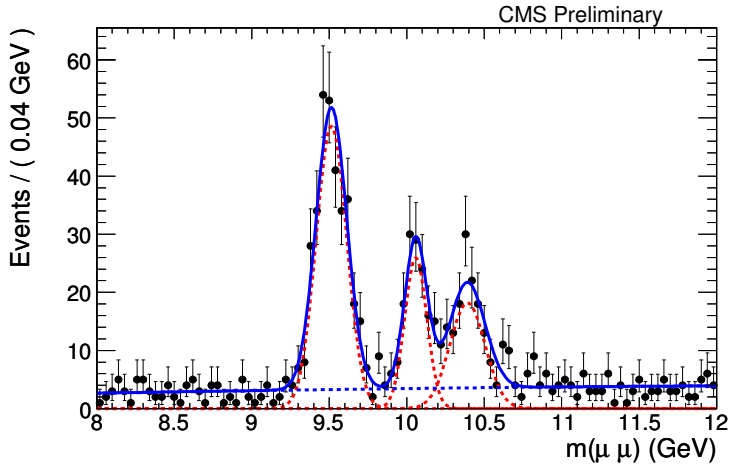

Figure 4: Dimuon invariant mass in the range $8 < m(\mu^+\mu^-) < 12$ GeV. The lines show the result of a fit, where the dashed line is the Υ component, the dotted line is the two-photon continuum, and the solid line is the sum of the two.

5.2 Υ Physics

The Υ photoproduction signal can be extracted by performing a fit to the dimuon invariant mass distribution in the range $8 < m < 12$ GeV. The $1S$, $2S$, and $3S$ Υ resonances are fitted to single Gaussians, while the sum of elastic and inelastic $\gamma\gamma \to \mu^+\mu^-$ contributions are fitted to a second order polynomial (Figure 4). For an assumed integrated luminosity of $100\,\mathrm{pb}^{-1}$ and the cross-section predicted from $STARLIGHT$, the three Υ resonances are clearly visible above the $\gamma\gamma$ continuum. The γp centre-of-mass energy for the selected events is $\langle W \rangle_{visible} = 537$ GeV.

With hundreds of events, further studies of Υ production, such as measuring t or η distributions, may be performed. While t cannot be measured directly, the p_T^2 of the Υ is expected to provide a good approximation. Preliminary studies with STARLIGHT signal samples confirm this, with the measured slope of the reconstructed p_T^2 distribution $b = (3.50 \pm 0.06)\,\mathrm{GeV}^{-2}$ in agreement with the generator-level value of $b = (4.03 \pm 0.04)\,\mathrm{GeV}^{-2}$.

6 Heavy Ion Interactions

In heavy ion collisions, the effective cross-section is enhanced over the pp case by a factor of Z^4 for $\gamma\gamma$ interactions (Z^2 for γA interactions), resulting in large event yields for relatively low integrated luminosities. A full simulation study has been performed using events generated with the STARLIGHT model, for an assumed Pb-Pb run of $0.5\,\mathrm{nb}^{-1}$ collected at $\sqrt{s} = 5.5$ TeV. The trigger selection requires identification of a $\mu^+\mu^-$ or e^+e^- pair of any energy, no significant activity within the forward hadronic calorimeter (covering $3 < |\eta| < 5$), and a neutron from the Coulomb breakup of the the ion detected in the ZDC.

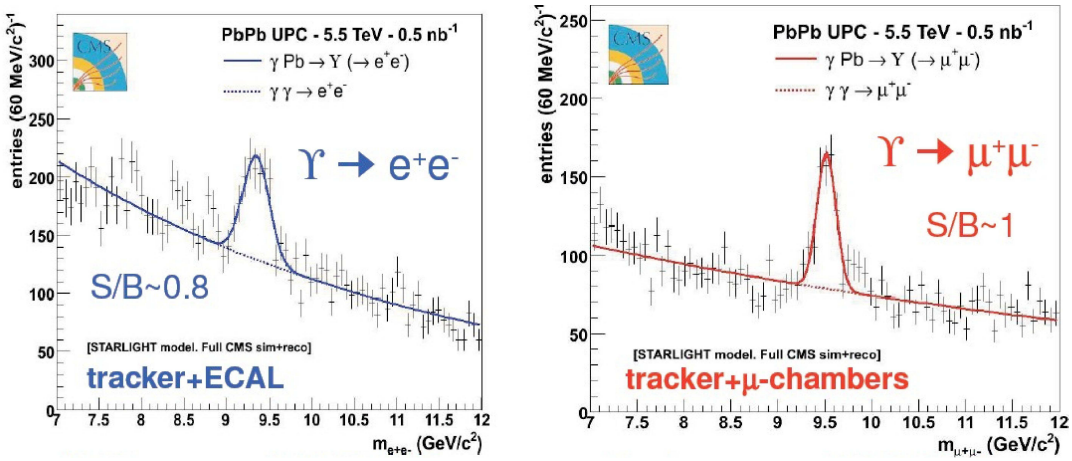

Figure 5: Dielectron (left) and dimuon (right) invariant masses in the range $7 < m(\mu^+\mu^-) < 12$ GeV. The lines show the result of a fit to the $\Upsilon(1S)$ signal and continuum background.

The residual non-photon exchange background is subtracted using a sample of like-sign dileptons. After the trigger selection and background subtraction are performed, a sample of ~ 180 $\Upsilon(1S) \to \mu^+\mu^-$ and ~ 220 $\Upsilon(1S) \to e^+e^-$ events are expected in $0.5\,\mathrm{nb}^{-1}$. As in the pp case, the good resolution in the dimuon channel should allow resolution of the $\Upsilon(2S)$ and $\Upsilon(3S)$ resonances (not included in the simulation used here). Systematic uncertainties on the Upsilon yields are estimated to be $\sim 10\%$, based on variations in the shape of the continuum background.

7 Conclusions

With $100\,\mathrm{pb}^{-1}$ of integrated luminosity at $\sqrt{s} = 14$ TeV, a large sample of $\gamma\gamma \to \mu^+\mu^-$ and $\gamma p \to \Upsilon p \to \mu^+\mu^- p$ events can be triggered and reconstructed in the CMS experiment, using a common selection for both samples. A smaller sample of $\gamma\gamma \to e^+e^-$ events will also be collected. With minimal pileup these events can be distinguished using exclusivity requirements, and the inelastic backgrounds reduced using forward detector vetos. The Υ sample will allow measurements of cross-sections and production dynamics at significantly higher energies than previous experiments. The $\gamma\gamma \to \ell^+\ell^-$ sample will serve as a calibration sample for studies of luminosity and lepton reconstruction. In Heavy Ion interactions, a significant signal for $\gamma A \to \Upsilon A^{(*)} \to \ell^+\ell^- A^{(*)}$ may be observed in both the $\mu^+\mu^-$ and e^+e^- channels in a nominal $0.5\,\mathrm{nb}^{-1}$ Pb-Pb run at $\sqrt{s} = 5.5\,\mathrm{TeV}$.

References

[1] CERN-LHCC-2006-01 CMS Collaboration

[2] Phys.Lett.B 328 (1994) 369-373, J. Ohnemus, T.F. Walsh, and P.M. Zerwas

[3] Phys.Rev.D50 (1994) 2335-2338 M. Drees, R.M. Godbole, M. Nowakowski, and S.D. Rindani

[4] Phys.Rev.D53 (1996) 2371-2379, G. Bhattacharya, Pat Kalyniak, and K.A. Peterson

[5] arXiv:0908.2020, J. de Favereau de Jeneret, et al.

[6] Phys.Rev.D78 (2008) 073005, O. Kepka, and C. Royon

[7] Phys.Rev.Lett.102 (2009) 222002 T. Aaltonen et al.

[8] Phys.Rev.Lett.81 (1998) 524-529 B. Abbott et al.

[9] Phys. Lett.B (2000) 483 C. Adloff, et al.

[10] arXiv:0903.4205 ZEUS Collaboration

[11] Nucl.Phys.B 229 (1983) 347, J.A.M. Vermaseren

[12] arXiv:0806.0302, M. Albrow, et al.

[13] Phys.Lett.B 679 (2009) 321-329, S. Afanasiev et al.

[14] hep-ph/0311164J. Nystrand and S. Klein

[15] hep-ph/0412096J. Nystrand and S. Klein

[16] J. Phys.G 23 (1997) 2069-2080 Angelis, A. L. S. and Panagiotou, A. D.

[17] AIP Conf. Proc. 867 (2006) 258-265 Grachov, Oleg A., et al.